Predicting Terrain Parameters for Physics-Based Vehicle Mobility Models from Cone Index Data

W. Huang[a*1], J.Y. Wong[b], J. Preston-Thomas[a], P. Jayakumar[c]

[a] ***National Research Council Canada, Ottawa, Ontario, Canada***
[b] ***Vehicle Systems Development Corporation, Toronto, Ontario, Canada***
[c] ***U.S. Army CCDC Ground Vehicle Systems Center, Warren, MI, USA***

Abstract

To provide terrain data for the development of physics-based vehicle mobility models, such as the Next Generation NATO Reference Mobility Model, there is a desire to make use of the vast amount of cone index (CI) data available. The challenge is whether the terrain parameters for physics-based vehicle mobility models can be predicted from CI data. An improved model for cone-terrain interaction has been developed that takes into account both normal pressure and shear stress distributions on the cone-terrain interface. A methodology based on Derivative-Free Optimization Algorithms (DFOA) has been developed in combination with the improved model to make use of continuously measured CI vs. sinkage data for predicting the three Bekker pressure-sinkage parameters, k_c, k_ϕ and n, and two cone-terrain shear strength parameters, c_c and ϕ_c. The methodology has been demonstrated on two types of soil, LETE sand and Keweenaw Research Center (KRC) soils, where continuous CI vs. sinkage measurements and continuous plate pressure vs. sinkage measurements are available. The correlations between the predicted pressure-sinkage relationships based on the parameters

[1] Corresponding author.

E-mail addresses: wei.huang@nrc-cnrc.gc.ca (W. Huang), vsdccanada@yahoo.ca (J.Y. Wong), jon.preston-thomas@nrc-cnrc.gc.ca (J. Preston-Thomas), paramsothy.jayakumar.civ@mail.mil (P. Jayakumar).

derived from continuous CI vs. sinkage measurements using the DFOA-based methodology and that measured were generally encouraging.

Keywords: Bekker-Wong terrain parameters, Bevameter, Cone index (CI), Cone-terrain interaction, Derivative-free optimization algorithms (DFOA), Normal pressure distribution, Shear stress distribution.

Nomenclature

B-W	Bekker-Wong
CI	cone index
CI_1 .. CI_6	cone index values at six penetration depths
CV	coefficient of variation
c_c	adhesion on the cone (metal)-terrain interface
D	diameter of a cone base or a circular plate
DFOA	derivative-free optimization algorithms
d	diameter of a portion of a cone that is at a distance h below the cone base
F_p	vertical resisting force offered by the vertical component of the normal pressure p on a cone surface
F_s	vertical resisting force offered by the vertical component of the shear stress s on a cone surface
H	height of a cone from cone base to the tip
h	height from cone base to where the cone diameter is d or $2r$
j	shear displacement
K	shear deformation parameter
K_c	shear deformation parameter on the cone (metal)-terrain interface
KRC	Keweenaw Research Center
k_c, k_ϕ	Bekker pressure-sinkage parameters
LETE	Land Engineering Test Establishment, Department of National Defence, Canada
NATO	North Atlantic Treaty Organization
NG-NRMM	Next-Generation NATO Reference Mobility Model
NRMM	NATO Reference Mobility Model
NTVPM	Nepean Tracked Vehicle Performance Model

NWVPM	Nepean Wheeled Vehicle Performance Model
n	exponent of the Bekker pressure-sinkage equation
PSO	particle swarm optimization
P-S	pressure-sinkage
p	pressure
p_1, p_2	pressure at a smaller plate size r_1, and larger plate size r_2, respectively, when r_1 and r_2 are dimensions of plates used in plate P-S tests, and the Bekker equation is used to estimate pressure at a given sinkage
R	radius of a cone base
R	coefficient of correlation
R^2	coefficient of determination
RMSD	root mean square deviation
RM0	a baseline model that relies on the Bekker equation to describe the relationship between p, z and r
RM1	an alternative model that relies on the Bekker equation to describe the relationship between p, z and r when $r>r_{min}$, and where pressure p changes linearly with plate size r when $r<r_{min}$
r	radius of a portion of a cone that is a distance h below the cone base, or radius of a circular plate
r_1, r_2	radius of the smaller and larger plates, respectively, of plates used in plate P-S tests
r_{min}	a transition plate size in the RM1 model
s	shear stress
W	the vertical force applied to a cone to cause the base to penetrate to a depth z

z	penetration depth of the bottom of a plate from the terrain surface, or penetration of a cone where the origin is set at the point where the cone base is flush with the terrain surface
z_1 .. z_6	six penetration depths at which CI values are measured
ϕ_c	angle of friction on the cone (metal)-terrain interface

1. Introduction

To provide terrain data for the development of physics-based vehicle mobility models, such as the Next Generation NATO Reference Mobility Model (NG-NRMM), there is a desire to make use of the vast amount of cone index (CI) data collected from various parts of the globe over many decades. To address this issue, a major challenge is to develop a method that can be used to derive, from CI data, the values of terrain parameters for physics-based vehicle mobility models, such as the Bekker-Wong (B-W) terrain parameters (Bekker, 1969; Wong, 2008, 2010). The complete set of B-W terrain parameters includes:

A. pressure-sinkage (P-S) parameters for various types of terrain (including mineral, organic and snow-covered terrains);

B. internal shear parameters for various types of terrain;

C. vehicle running gear surface-terrain shear parameters (e.g., rubber-terrain shear parameters for evaluating the traction of rubber tires or rubber tracks) for various types of terrain;

D. vehicle belly (metal)-terrain shear parameters (for analyzing vehicle belly-terrain interaction, when the vehicle belly is in contact with the terrain surface) for various types of terrain;

E. parameters for characterizing the response of various types of terrain to repetitive normal and shear loadings.

B-W terrain parameters have been used in the development of physics-based simulation models, such as NTVPM and NWVPM for evaluating the cross-country performance of tracked and wheeled vehicles, respectively (Wong, 2008, 2010; Wong et al., 2018, 2019). These simulation models have been employed in assisting vehicle manufacturers in the development

of new products (Wong, 1992, 1995), as well as governmental agencies and industry in the evaluation of off-road vehicle performance (Wong, 2006, 2008; Wong et al., 2015).

A pioneering attempt to establish a relationship between CI and the Bekker P-S parameters was made by Janosi (Janosi, 1959). However, it did not take into account the shear stress on the cone-terrain interface.

In this paper, an improved model for cone-terrain interaction that considers both the normal pressure and shear stress distributions on the cone-terrain interface is proposed. The functional relationship between CI and two groups of B-W terrain parameters, namely the Bekker P-S parameters and the cone (metal)-terrain shear parameters, is developed. The general features of the improved model are substantiated with two sets of terrain data where records of continuous measurements of both CI and the plate pressure vs. sinkage were available. The first set is referred to as the LETE sand data and was measured in 1981 for the Department of National Defence of Canada (Wong, 1981). The second set was measured in 2018 at the Keweenaw Research Center (KRC) in Michigan, USA, under contract to the U.S. Army, and is thus referred to as the KRC soil data (Gerth et al., 2019).

Methods for predicting the values of the Bekker P-S parameters and the cone-terrain shear parameters from measured CI data are explored. A methodology selected for this study uses derivative-free optimization algorithms (DFOA) with continuous CI vs. sinkage measurements as input and uses the improved cone-terrain interaction model to predict the Bekker P-S parameters and the cone-terrain shear parameters. The results of applying the DFOA-based methodology to predicting the Bekker P-S parameters and the cone-terrain shear parameters based on the LETE sand data and the KRC soil data are presented. The methodology achieves positive results in terms of its ability to predict these parameters from CI data.

2. An Improved Cone-Terrain Interaction Model

As noted previously, a relationship between CI and the Bekker P-S parameters was established by Janosi (Janosi, 1959). This relationship was based on the assumptions that:

A. on the cone-terrain interface, there was only vertical pressure present and the shear stress on the interface was ignored. In reality, in addition to normal pressure, shear-stress is present on the cone (metal)-terrain interface;
B. the denominator of k_c in the pressure-sinkage equation used in Janosi's analysis was the diameter of the cone base. In the original Bekker pressure-sinkage equation, the denominator of k_c is, however, the radius of the cone base.

With the standard circular cone having a base area of 0.5 in.^{2} and a cone angle of 30°, the relationship between CI and the Bekker P-S parameters is given by Janosi as follows (Janosi, 1959; also described in Bekker, 1969):

$$CI = 1.625\{\frac{k_c}{(n+1)}[(z+1.5)^{n+1} - z^{n+1}] + 0.517\,k_\phi[\frac{(z+1.5)^{n+2}}{(n+1)(n+2)} + \frac{z^{n+2}}{n+2} - \frac{(z+1.5)\,z^{n+1}}{n+1}]\} \qquad (2\text{-}1)$$

where k_c, k_ϕ, and n are the Bekker P-S parameters; z is the penetration depth of the cone with the origin set at the point where the cone base is flush with terrain surface.

It should be noted that the cone index was first developed in the United States and that CI represents the force in lb required to push the cone into the terrain divided by the standard cone base area of 0.5 in.^{2}. Consequently, CI, as calculated using Equation (2-1), would have the U.S. customary unit of psi (lb/in.^{2}). However, as a common practice in the military field, CI is considered as an index and no unit is attached to it. Since CI was originally derived using the U.S. customary units, SI units are not always used in this paper.

As shown in Figure 2-1 for a set of LETE sand data, there is a substantial difference between the measured values of CI and the calculated (predicted) values of CI obtained using Equation (2-1) with k_c = 32 lb/in.$^{n+1}$ (102 kN/m^{n+1}), k_ϕ = 42.2 lb/in.$^{n+2}$ (5,301 kN/m^{n+2}), and n = 0.79 (Wong, 1981).

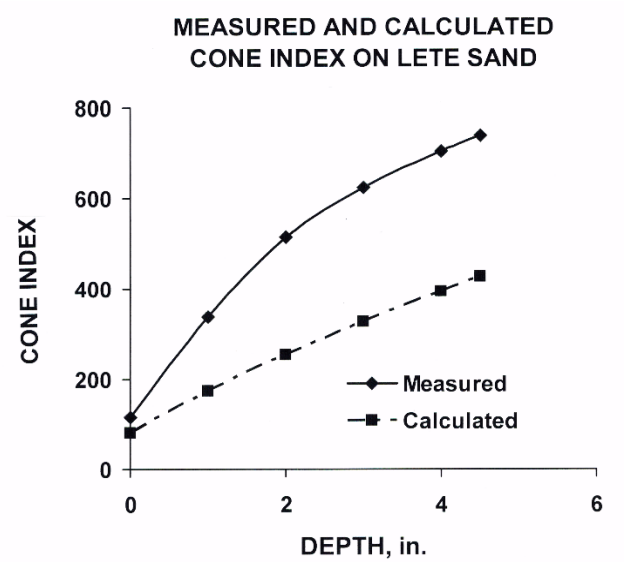

Figure 2-1. Comparison of the measured values of CI and the calculated values of CI from the Bekker P-S parameters obtained using the Janosi equation for LETE sand.

In view of the issues concerning the Janosi equation noted above, an improved model of cone-terrain interaction, in which both the normal pressure and shear stress on the cone-terrain interface are considered, is shown in Figure 2-2.

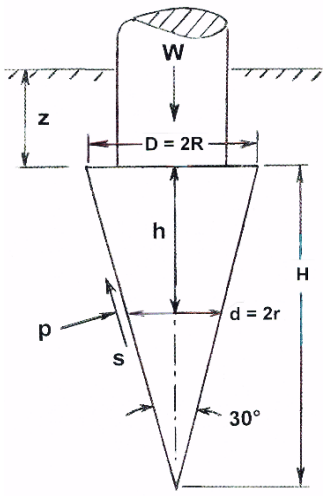

Figure 2-2. An improved model of cone-terrain interaction taking into account both normal pressure and shear stress on the interface.

The normal pressure p at a depth $z + h$ from the terrain surface is assumed to follow the original Bekker pressure-sinkage equation,

$$p = \left(\frac{k_c}{r} + k_\phi\right)(z+h)^n \tag{2-2}$$

where k_c, k_ϕ and n are the Bekker P-S parameters, as noted previously; r is the radius of the cone base at a depth of $z + h$ from the terrain surface shown in Figure 2-2, and is expressed by

$$r = R(H-h)/H \tag{2-3}$$

where R is the radius at the base of the cone and H is the height of the cone.

The shear stress s on the cone-terrain interface at a depth of $z + h$ from the terrain surface is assumed to follow the Janosi and Hanamoto equation (Janosi and Hanamoto, 1961):

$$s = (c_c + p\tan\phi_c)(1-e^{-j/K}) = (c_c + p\tan\phi_c)(1-e^{-[(z+h)/\cos 15^\circ K_c]}) \tag{2-4}$$

where c_c, ϕ_c, and K_c are the adhesion, angle of friction, and shear deformation parameter on the cone (metal)-terrain interface, respectively; $(z+h)/\cos 15°$ is the shear displacement of the point on the cone surface at a depth of $z+h$ from the terrain surface.

The vertical resisting force F_p offered by the vertical component of the normal pressure p on the cone surface is expressed by

$$F_p = \int_0^H p \times 2\pi\, r\,(dh/\cos 15°)\sin 15° = 2\pi \tan 15° \int_0^H (\frac{k_c}{r} + k_\phi)(z+h)^n\, r dh$$

$$= 2\pi \tan 15° \int_0^H (k_c + r\,k_\phi)(z+h)^n\, dh = 2\pi \tan 15° \int_0^H [(k_c + R(1-h/H)\,k_\phi](z+h)^n\, dh \qquad (2\text{-}5)$$

The vertical resisting force F_s offered by the vertical component of the shear stress s on the cone surface is expressed by

$$F_s = \int_0^H s \times 2\pi\, r\,(dh/\cos 15°)\cos 15° = 2\pi \int_0^H (c_c + p\tan\phi_c)(1 - e^{-[(z+h)/\cos 15° K_c]})\, r dh$$

$$= 2\pi \int_0^H [c_c\, r + (k_c + r\,k_\phi)(z+h)^n \tan\phi_c](1 - e^{-[(z+h)/\cos 15° K_c]})]\, dh$$

$$= 2\pi \int_0^H \{c_c\, R(1-h/H) + [k_c + R(1-h/H)\,k_\phi](z+h)^n \tan\phi_c\}(1 - e^{-[(z+h)/\cos 15° K_c]})\, dh \qquad (2\text{-}6)$$

The force W applied to the cone is balanced by the sum of the vertical resisting forces F_p and F_s. Based on the new model described above, the relationship between the cone index CI and the Bekker P-S parameters and cone-terrain shear parameters, for a circular cone with base radius R, is expressed by

$$CI = \frac{W}{\pi R^2} = \frac{F_p + F_s}{\pi R^2} = f(k_c, k_\phi, n, c_c, \phi_c, K_c, z) \qquad (2\text{-}7)$$

With the functional relationship between CI and the Bekker P-S parameters and cone-terrain shear parameters established by Equation (2-7), it is relatively straightforward to calculate the value of CI from the values of parameters k_c, k_ϕ, n, c_c, ϕ_c, and K_c. However, the reverse process of deriving the values of parameters k_c, k_ϕ, n, c_c, ϕ_c, and K_c from the values of CI is a very challenging task.

A. Conceptually, if CI values measured at six penetration depths (or more) are available, then the values of the six parameters, k_c, k_ϕ, n, c_c, ϕ_c, and K_c, could, in principle, be determined by solving the following six simultaneous equations:

$CI_1 = f(k_c, k_\phi, n, c_c, \phi_c, \text{and } K_c, z_1)$

$CI_2 = f(k_c, k_\phi, n, c_c, \phi_c, \text{and } K_c, z_2)$

$CI_3 = f(k_c, k_\phi, n, c_c, \phi_c, \text{and } K_c, z_3)$

$CI_4 = f(k_c, k_\phi, n, c_c, \phi_c, \text{and } K_c, z_4)$

$CI_5 = f(k_c, k_\phi, n, c_c, \phi_c, \text{and } K_c, z_5)$

$CI_6 = f(k_c, k_\phi, n, c_c, \phi_c, \text{and } K_c, z_6)$

However, this approach is based on the assumptions that

(a) the terrain is homogeneous within the sinkage range used in the study, such as from z_1 to z_6;

(b) the pressure-sinkage relationship and the vertical force on the cone base can be represented by the equations for radius from 0 (or close to 0) at the cone tip to that of the cone base with radius R.

B. Upon a review of many potential methodologies, the methodology based on DFOA is selected to derive the values of parameters k_c, k_ϕ, n, c_c, ϕ_c, and K_c from measured CI values. This approach will be described in detail in Section 3.

C. As mentioned previously, two groups of continuously measured CI and P-S data are available, one for LETE sand, and the other for mineral terrains obtained by KRC. The

application of the DFOA to these two groups of data for deriving the Bekker P-S parameters and the cone-terrain shear parameters from measured CI-sinkage data will be presented in Section 4.

3. Optimization Methods Used to Derive the Values of the Bekker Pressure-Sinkage Parameters and the Cone-Terrain Shear Parameters from Cone Index Measurements

3.1. Derivative-Free Optimization Algorithms

Many randomized heuristic derivative-free optimization algorithms can be used to iteratively tune a model for promising search areas and paths to obtain the best solutions. Particle Swarm Optimization (PSO) was used to generate optimized values for the Bekker P-S parameters and the cone-terrain shear parameters from the measured CI-sinkage data and the measured plate P-S data in the learning process, and from the measured CI-sinkage data in the prediction process. The details of the learning process and the prediction process of PSO will be described in Sections 3.3.1 and 3.3.2, respectively.

Particle Swarm Optimization was introduced in the mid-1990s (Kennedy and Eberhart, 1995; Kennedy, 1997; Shi and Eberhart, 1998; Kennedy and Eberhart, 2001). It was inspired by the ability of flocks of birds, schools of fish, and herds of animals to adapt to their environment, find rich sources of food, and avoid predators by implementing an “information sharing” strategy, hence, gaining an evolutionary advantage. The methodology is based on the observations of sociologist E.O. Wilson (1975), who, on the subject of fish schooling, said, “In theory at least, individual members of the school can profit from the discoveries and previous experience of all other members of the school during the search for food. This advantage can become decisive, outweighing the disadvantages of competition for food items, whenever the resource is unpedictably distributed in patches.” On these observations, Kennedy and Eberhart (1995) said “this statement suggests that social sharing of information among conspeciates offers an evolutionary advantage: this hypothesis was fundamental to the development of particle swarm optimization.”

PSO is a computational method in which a swarm of “particles” is modelled in a way that simulates the behaviour of a swarm of bees searching for nectar over a wide range of territory. In the application described here, each particle in the swarm is “flying” in a multiple-dimensional space with a specific vector for each of the Bekker P-S parameters and each of the cone-terrain shear parameters. The adjacent particles all have their own separate vectors. The quality of the fit between the measured data and fitted equation is evaluated for each of the particles in the swarm using the particle’s vector and the improved cone-terrain interaction model. PSO optimizes a problem by following an iterative procedure to improve a candidate solution. In this case, a decision is made about how to move a particle forward to the next step in the iteration in the same way that bees make decisions about where to fly next – based on their own experience, and on the social behaviour of the swarm. The process stops when further searching does not yield significant improvements in the quality of the solution. PSO is designed to find, generate, or select a search method that may provide a sufficiently good solution to an optimization problem, especially with incomplete or imperfect information. It does not require that the optimization problem be differentiable.

3.2. Methods to Limit the Predicted Pressure using the Bekker Equation When the Plate Radius is Approaching Zero

The Bekker equation was developed to make plate-size-dependent interpolations or extrapolations of the compressive strength of terrain from measurements made with plates of a size that approximates the tire contact area or track link contact area of a vehicle of interest. For circular contact areas it uses the plate radius r for characterizing the size of the contact area.

In the improved cone-terrain interaction model described in Section 2, the Bekker equation has been used to describe the normal pressure distribution on the cone surface. In cases where k_c and k_ϕ are both positive, the Bekker equation estimates that the pressure will approach infinity as the size of the contact area, (i.e., radius r) approaches zero at the tip of the cone.

There is a high degree of uncertainty about whether P-S measurements made with bevameter plates of 3.75 cm (1.5 in.) and 5 cm (2 in.) in radius for the LETE sand, or 4 in. (10 cm) and 6 in. (15 cm) in diameter for the KRC soils, can be accurately extrapolated to estimate the pressure on a cone where the radius of the contact area varies from zero (or close to zero) at the tip to 0.4 in. (1 cm) at the base.

In the process of investigating the effectiveness of the DFOA-based methodology on predicting the Bekker P-S parameters from CI measurements, the improved cone-terrain interaction model that was described in Section 2 and uses the Bekker equation was designated as the “RM0” model.

As described in Section 2, this model likely has substantial limitations in its ability to correctly estimate the normal pressure distribution on a cone surface due to the small dimensions of the cone, particularly near the cone tip. As a result, an alternative model, RM1, was defined to investigate how the modification of the pressure-sinkage relationship in the region where the equivalent plate sizes are small would affect the prediction effectiveness. The baseline and the alternative model are thus as follows:

Baseline model - RM0 (the Bekker equation): $p = (k_c/r+k_\phi)z^n$

Alternative model - RM1 (tangent at $r=r_{min}$): $p = (k_c/r_{min}+k_\phi)z^n + (r_{min}-r)k_c/r_{min}^2\, z^n$ *when* $r < r_{min}$

In the baseline RM0 model, the pressure p is defined from the sinkage z, the P-S parameters, k_c, k_ϕ and n, and the plate radius r. This is the Bekker equation with its asymptote approaching infinity when the plate size approaches zero.

In the RM1 model, when the plate radius r is less than a defined transition value r_{min}, the pressure p changes linearly with plate size, with the relationship between pressure at a given

sinkage and plate size being tangent to that of the RM0 model at r=r_{min}. When the plate radius r is above r_{min}, the RM0 model applies.

It should be noted that when k_c is zero, the RM1 model is the same as the RM0 model and there is no requirement to search for a value of r_{min}.

When k_c is not zero, the DFOA methodology automatically finds a value of r_{min} for each of the measured terrain data sets (where a terrain data set consists of a measured CI-sinkage relationship and the two measured plate pressure-sinkage relationships) that provides the best overall fit between the measured and predicted CI-sinkage relationships and the measured and predicted plate P-S relationships.

If r_{min} is higher than the radius of the larger of the two plates used in the P-S tests, the pressure p will change linearly with plate size, along the line through (p_1, r_1) and (p_2, r_2), where r_1 and r_2 are the dimensions of the smaller and larger plates used in the plate P-S tests, and p_1 and p_2 are the corresponding pressures estimated by the Bekker equation for those two plate sizes.

The DFOA methodology automatically finds a value of r_{min} for each of the measured terrain data sets that provides the best overall fit between the measured and predicted CI-sinkage relationships and the measured and predicted plate P-S relationships.

3.3. The DFOA-Based Methodology to Predict the Bekker Pressure-Sinkage Parameters and the Cone-Terrain Shear Parameters from Cone Index Measurements

As described in Section 3.1, particle swarm optimization (PSO) is the DFOA-based methodology used to predict the Bekker P-S parameters and the cone-terrain shear parameters from CI-sinkage measurements. It should be pointed out that for this study using the LETE sand data and the KRC soil data, among the cone-terrain shear parameters, c_c, ϕ_c, and K_c, the shear deformation parameter K_c has been found to have little effect on the optimization process.

Therefore, the methodology used in this study involves the modeling of a swarm of particles flying through only a 5-dimensional space, searching for the combination of k_c, k_ϕ, n, c_c and ϕ_c that provides the best overall fit of the improved cone-terrain interaction model to the measured data. The methodology simulates the behaviour of a swarm of bees flying in their territory and searching for nectar.

This DFOA-based methodology is shown in the flow chart in Figure 3-1. It has two principal parts – the first is a learning process shown by the dashed-red-line box, and the second is a prediction process shown by the dashed-green-line box. Each of the learning and prediction processes makes use of a common central core. Two ovals in the figure show the inputs for the two processes, two more ovals show the outputs for the processes, and the circles show the points where the processes end.

3.3.1. The DFOA-Based Learning Process

The DFOA-based learning process begins at the top right of the Learning Process box in Figure 3-1 by reading continuously measured CI-sinkage relationships, cone sizes, measured pressure-sinkage (P-S) relationships and plate sizes, and any measured shear stress-shear displacement relationships, shear device dimensions or shear strength relationships that may be available for cone (metal)-terrain shearing. If no measured shear data is available, as was the case with both the LETE sand and KRC soil data sets, estimates of the shear strength parameters are made.

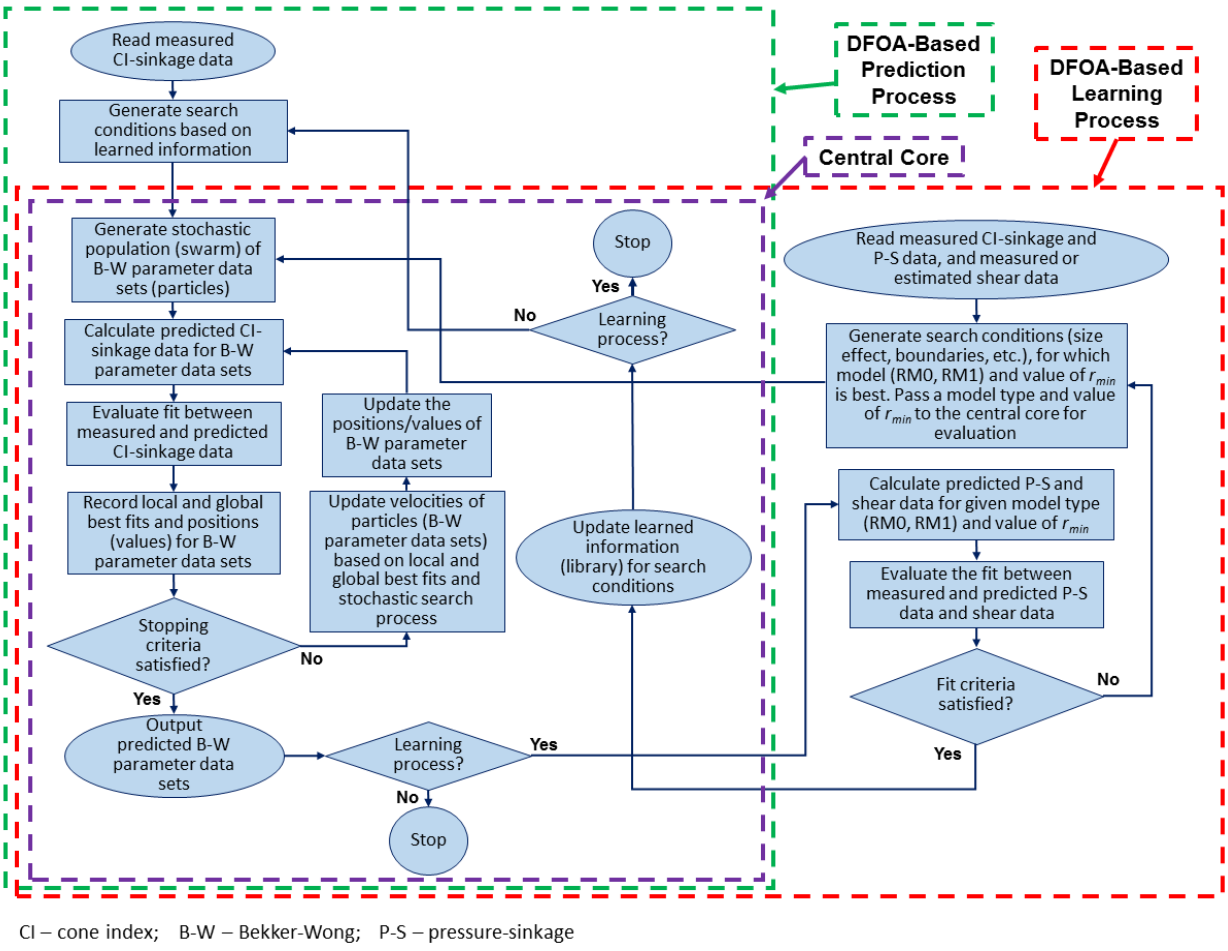

Figure 3-1 Flow chart showing the DFOA-based learning process, and the DFOA-based prediction process.

A search is then initiated to find the best fit between the measured and predicted plate P-S relationships. For the RM1 model, this also includes a search to find the best value of r_{min}, the plate radius at which the transition is made between the Bekker equation and the pressure-limiting function of the model.

The search for the best value of r_{min} is controlled by the column of boxes on the right side of the Learning Process. This is an outer search loop that makes use of an inner search loop that is entirely inside the central core. In the process of conducting this search, a specific value of r_{min} is passed to the central core.

As noted previously, in this study the central core focuses on finding a set of five parameters, k_c, k_ϕ, n, c_c, and ϕ_c, that provide the best fit between the improved cone-terrain interaction model and the measured CI-sinkage and plate P-S relationships, for the specified model type and specified value of r_{min}. These parameters are passed back to the outer search loop in the box labeled "Calculate predicted P-S and shear data for a given model type and value of r_{min}." After the predicted P-S and shear parameters are calculated, the fit between the predicted and measured data is evaluated. If the fit criteria are not completely satisfied, control is returned to the "Generate search…" box to define a new value of r_{min}. The new value is then sent to the central core for processing. When all the outer-loop fit criteria have been satisfied, control is passed to the oval in the middle right of the central core to update the information library with the results of the learning process for the given input data. The learning process then stops, and the methodology proceeds to the prediction process.

3.3.2. The DFOA-Based Prediction Process

As shown at the top left of Figure 3-1, the DFOA-based prediction process starts by reading in a continuous CI-sinkage relationship for which a corresponding set of predicted parameters k_c, k_ϕ, n, c_c, and ϕ_c need to be found, and where the relationships are defined by the improved cone-terrain interaction model. As a result of the already completed learning process, the value of r_{min} is defined (if the RM1 model is being used).

A large swarm of particles is generated in which each particle contains a complete parameter data set – a specific combination of k_c, k_ϕ, n, c_c, and ϕ_c. This is a vector that defines the particle "position". The improved cone-terrain interaction model is then used to calculate the CI-sinkage relationship for each of the particles in the swarm. The search process then evaluates the fit between the measured and predicted CI-sinkage relationships for each of the particles in the swarm. Note is made of the global fit for all particles (i.e., the best prediction based on social

experiences and on the local fit (i.e., the best fit based on self-experiences). Each particle in the search space adjusts its “flying” through the 5-dimensional search space according to its own flying-experience (i.e., where it has been in the search space, and what the fit of the improved cone-terrain interaction model has been at the points in that space), as well as the flying-experiences of the other particles.

If the process has converged to a solution, then the predicted parameters are output. Otherwise, the values of the parameters k_c, k_ϕ, n, c_c, and ϕ_c in each of the particles are changed.

The rate at which the values change is referred to as particle velocity. The position and velocity of each of the particles in the swarm is changed in accordance with the DFOA algorithms. Once a new swarm position has been defined, control is passed back to a higher position in the search loop for calculating the predicted CI-sinkage data for the pressure-sinkage and the cone-terrain shear parameter data sets. This search continues until the search criteria are satisfied.

4. Applying the DFOA-Based Methodology to the Measured Sample Terrain Data

The methodology based on Derivative-Free Optimization Algorithms (DFOA) described in Section 3 is used together with the improved cone-terrain interaction model described in Section 2 to predict the Bekker P-S parameters k_c, k_ϕ and n, and the cone-terrain shear parameters c_c, and ϕ_c for selected sets of measured CI data. Two sets of measured CI data were used in this assessment. The first was a set of LETE sand CI data measured in 1981. The second was a set of soil CI data from the Keweenaw Research Center (KRC) measured in 2018.

4.1. Predictions Using the LETE Sand Data

Four measurements of CI vs. sinkage relationships were made on LETE sand, and they are designated LS_1, LS_2, LS_3 and LS_4 here. Five pairs of plate pressure-sinkage measurements were also made on LETE sand. Each pair includes a measurement with a 3.75 cm (1.5 in.)-radius plate and a measurement with a 5 cm (2.5 in.)-radius plate. These five measured P-S data sets are designated LS_A, LS_B, LS_C, LS_D and LS_E here. The LETE sand CI and P-S measurements were all made on June 12, 1981 on a test site where the terrain strength was expected to be relatively uniform.

Applying the DFOA-based methodology to each of the four measured LETE sand CI-sinkage relationships results in a set of predicted Bekker P-S parameters and cone-terrain shear parameters, as shown in Table 4-1. Each set of terrain parameters includes the three Bekker P-S parameters, k_c, k_ϕ and n, and the two shear parameters, c_c and ϕ_c, that describe the cohesion and friction, respectively, of the cone (metal)-terrain shear strength.

Table 4-1
Predicted Bekker P-S parameters and cone-terrain shear parameters based on measured LETE sand CI data.

Data Set	k_c		k_ϕ		n	c_c		ϕ_c,
	kN/m^{n+1}	lb/in.$^{n+1}$	kN/m^{n+2}	lb/in.$^{n+2}$		kPa	psi	deg
LS_1	80.14	30.2	4727.2	45.25	0.74	0	0	12.5
LS_2	73.17	53.03	2812.8	51.78	0.562	0	0	10
LS_3	90.41	40.5	4075	46.36	0.693	0	0	10.03
LS_4	96.28	38.63	4551.1	46.38	0.723	0	0	10.78

Predicted Cone Index-sinkage relationships were obtained with the improved cone-terrain interaction model and the terrain parameters listed in Table 4-1 that were obtained by applying the methodology based on Derivative-Free Optimization Algorithms to the measured Cone Index-sinkage relationships.

Predicted Cone Index-sinkage relationships and measured Cone Index-sinkage relationships for the four CI cases (LS_1 to LS_4) are shown together in Figure 4-1. The measured relationships are shown with dashed lines, and the predicted relationships are shown with solid lines.

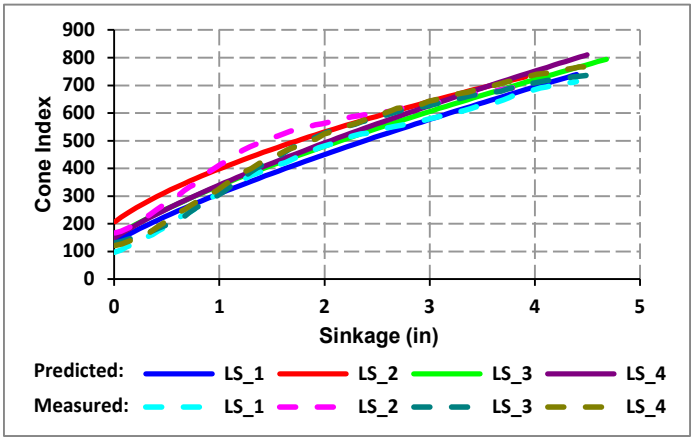

Figure 4-1. Measured and predicted Cone Index-sinkage relationships for the four LETE sand CI data sets.

The LS_1 set of predicted Bekker P-S parameters in Table 4-1 can be used together with the Bekker Equation to predict the pressure-sinkage relationship for a 3.75 cm (1.5 in.)-radius plate, and that is shown as a dark blue solid line in Figure 4-2(a). They can also be used together to predict the P-S relationship on a 5 cm (2.5 in.)-radius plate, and that is shown as a dark blue solid line in Figure 4-2(b). Corresponding predictions of plate pressure-sinkage relationships can be made using the parameters shown in Table 4.1 for the LS_2, LS_3 and LS_4 CI-sinkage measurements, and those relationships are also shown as solid lines in Figure 4-2(a) and (b). The five measured P-S relationships (LS_A to LS_E) for the 3.75 cm (1.5 in.)-radius plate are shown as dashed lines in Figure 4-2(a), and the five measured P-S relationships for the 5 cm (2. in.) -radius plate are shown as dashed lines in Figure 4-2(b).

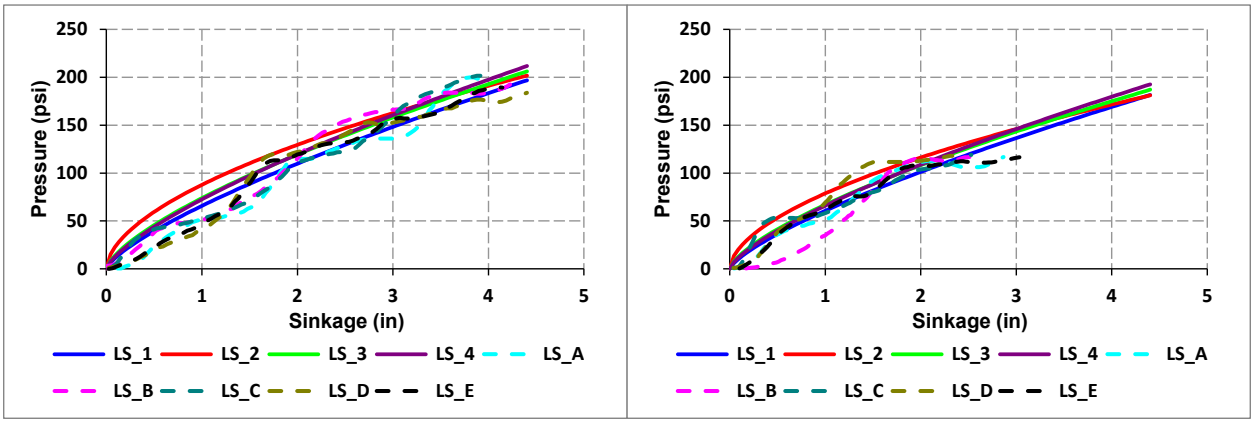

(a) (b)

Figure 4-2. Measured (LS_A to LS_E shown with dashed lines) and predicted (LS_1 to LS_4 shown with solid lines) P-S relationships for LETE sand with: (a) plate radius r = 3.75 cm (1.5 in.); (b) plate radius r = 5 cm (2 in.).

To evaluate the goodness of fit between the predicted and measured LETE sand P-S relationships, values of the coefficient of correlation R, coefficient of determination R^2, root mean square deviation (RMSD) and the coefficient of variation (CV) are shown in Table 4-2. The first five rows of the table are for predicted P-S relationships that were derived from the measured LS_1 CI-sinkage relationship. The first row compares the LS_1 predicted P-S relationship against the measured LS_A P-S relationship for each of the two plate sizes used in

the experiments. The second row compares the LS_1 predicted P-S relationship with the measured LS_B P-S relationship for each of the two plate sizes used in the experiments. The next three rows provide corresponding evaluations of the LS_1 predicted P-S relationship with the LS_C, LS_D and LS_E measurements. The remainder of the table provides corresponding comparisons of the LS_2, LS_3 and LS_4 predictions with the LS_A to LS_E measurements. With four predictions (arising from the four CI-sinkage measurements), and five pairs of plate P-S measurements, there are twenty comparisons in total.

Table 4-2
R, R^2, RMSD and CV between LETE sand measured P-S relationships and predicted P-S relationships derived from measured CI data.

Cone Index Data Used for Prediction	Measured Pressure-Sinkage Data for Comparison	R = 3.75 cm (1.5 in.)					R = 5 cm (2.5 in.)				
		R	R^2	RMSD kPa	RMSD psi	CV	R	R^2	RMSD kPa	RMSD psi	CV
LS_1	LS_A	0.9874	0.975	102.5	14.87	0.1457	0.9668	0.9346	91.7	13.3	0.1786
LS_1	LS_B	0.9839	0.968	97.63	14.16	0.124	0.9733	0.9474	144.6	20.97	0.3173
LS_1	LS_C	0.9846	0.9695	91.42	13.26	0.1253	0.9777	0.9559	64.53	9.36	0.1299
LS_1	LS_D	0.9771	0.9548	96.04	13.93	0.1258	0.9724	0.9455	80.19	11.63	0.1532
LS_1	LS_E	0.991	0.982	74.46	10.8	0.1013	0.9704	0.9417	93.7	13.59	0.1718
LS_2	LS_A	0.9813	0.963	198.4	28.78	0.2819	0.9736	0.948	204.3	29.63	0.3979
LS_2	LS_B	0.9799	0.9602	142.3	20.64	0.1808	0.9706	0.942	264.3	38.33	0.5799
LS_2	LS_C	0.9728	0.9463	164.9	23.92	0.226	0.9787	0.9579	174.9	25.37	0.352
LS_2	LS_D	0.9803	0.9611	164.8	23.9	0.2158	0.9784	0.9573	126.3	18.32	0.2412
LS_2	LS_E	0.9896	0.9794	156.9	22.75	0.2133	0.9811	0.9625	204.6	29.67	0.3752
LS_3	LS_A	0.9862	0.9727	135.5	19.65	0.1925	0.9691	0.9391	137.3	19.92	0.2675
LS_3	LS_B	0.9836	0.9674	95.01	13.78	0.1207	0.973	0.9467	187.1	27.14	0.4106
LS_3	LS_C	0.982	0.9643	105.5	15.3	0.1445	0.9783	0.9571	106.5	15.44	0.2142
LS_3	LS_D	0.9786	0.9577	118.9	17.25	0.1558	0.9745	0.9496	71.5	10.37	0.1366
LS_3	LS_E	0.9913	0.9826	98.73	14.32	0.1342	0.9735	0.9478	141.8	20.57	0.2601
LS_4	LS_A	0.987	0.9742	133.4	19.35	0.1896	0.9676	0.9363	137.8	19.98	0.2684
LS_4	LS_B	0.9838	0.9679	91.29	13.24	0.116	0.9732	0.9472	181.6	26.34	0.3985
LS_4	LS_C	0.9837	0.9677	100.4	14.56	0.1375	0.9779	0.9564	106.3	15.42	0.2139
LS_4	LS_D	0.9777	0.9559	123.3	17.88	0.1615	0.9732	0.947	69.15	10.03	0.1321
LS_4	LS_E	0.9911	0.9823	98.94	14.35	0.1346	0.9715	0.9439	144.7	20.98	0.2652

4.2. Predictions Using the KRC Soil Data

Measurements of Cone index-sinkage relationships and P-S relationships for two different plate sizes were made on eight different sites, designated KRC_1, KRC_2, KRC_3, KRC_4, KRC_7, KRC_9, KRC_24 and KRC_25. An effort was made to provide uniform terrain strength within a given site, but there was no expectation that the eight sites would have similar terrain strengths. There was a single CI-sinkage relationship measured on each of the eight sites, and a single pair of plate P-S relationships measured with 4 in. (10 cm)-diameter and 6 in. (15 cm)-diameter plates for each of the eight sites.

Applying the DFOA-based methodology to the measured KRC_1 CI-sinkage relationship results in a set of predicted pressure-sinkage and cone-terrain shear parameters, as shown in Table 4-3. Again, each set of terrain parameters includes the three P-S parameters, k_c, k_ϕ and n, and the two shear parameters, c_c and ϕ_c, that describe the cohesion and friction, respectively, of the cone (metal)-terrain shearing strength. Each remaining row of the table (KRC_2 to KRC_25) shows the corresponding predicted parameter set that was obtained from the measured CI-sinkage relationship made on that site.

Table 4-3
Predicted Bekker pressure-sinkage parameters and cone-terrain shear parameters based on measured KRC soil CI data.

Data Set	k_c		k_ϕ		n	c_c		ϕ_c,
	kN/m^{n+1}	lb/in.$^{n+1}$	kN/m^{n+2}	lb/in.$^{n+2}$		kPa	psi	deg
KRC_1	42	27.36	885.18	14.648	0.591	1	0.15	10
KRC_2	96.84	28.33	673.67	5.005	0.809	0	0	15.82
KRC_3	0	0	1948.9	42.791	0.514	0	0	14.37
KRC_4	1	0.318	2571.3	20.789	0.786	0	0	14.07
KRC_7	0.89	1.21	1417.3	48.892	0.391	1	0.15	9.14
KRC_9	8.91	10.26	1881.3	55.011	0.436	0	0	17.76
KRC_24	22.02	6.66	2273.7	17.462	0.8	0	0	11.18
KRC_25	0	0	1628.8	26.953	0.591	0	0	21.22

The measured CI-sinkage relationship for the KRC_1 site is shown as a dashed red line in Figure 4-3(a). The KRC_1 set of predicted terrain parameters can be used with the improved cone-terrain interaction model to obtain a prediction of the CI-sinkage relationship for the KRC_1 site. This prediction is shown as a solid blue line in Figure 4-3(a). Corresponding comparisons of the measured and predicted CI-sinkage relationships for the other seven KRC soil sites are shown in Figure 4-4(a) to Figure 4-10(a).

The KRC_1 set of predicted terrain parameters in Table 4-3 can be used together with the Bekker Equation to predict the P-S relationship for a 4 in. (10 cm)-diameter plate, and that is shown as a blue solid line in Figure 4-3(b). They can also be used together to predict the P-S relationship on a 6 in. (15 cm)-diameter plate, and that is shown as a green solid line in Figure 4-3(b). The measured P-S relationships for the two plate sizes in KRC_1 are shown with dashed lines in the same figure. Figure 4-4(b) to Figure 4-10(b) show corresponding comparisons of the predicted and measured P-S relationships for the same two plate sizes using the P-S parameters for the other KRC soil CI-sinkage measurements.

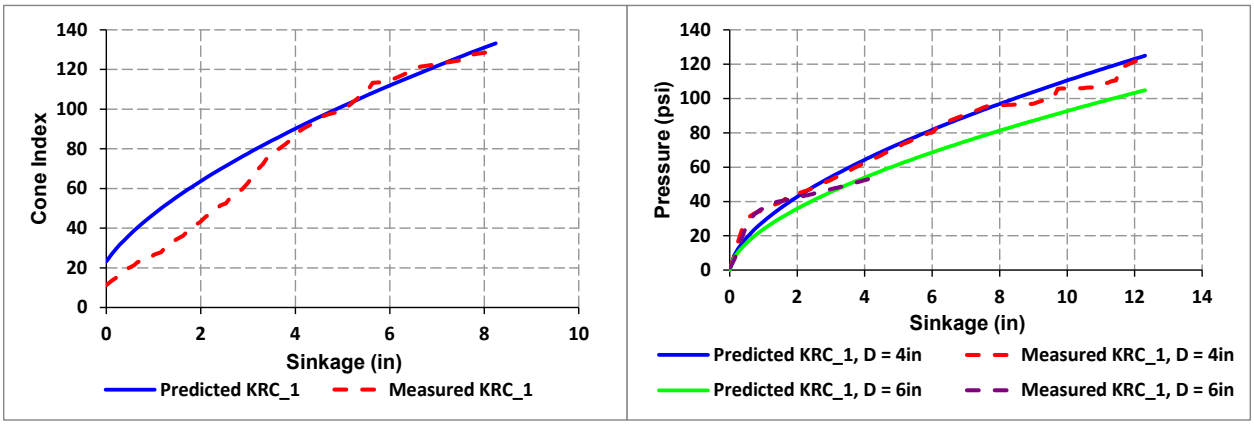

(a) (b)

Figure 4-3. KRC_1 measured and predicted: (a) CI-sinkage relationships; (b) P-S relationships for 4 in. (10 cm) and 6 in. (15 cm)-diameter plates.

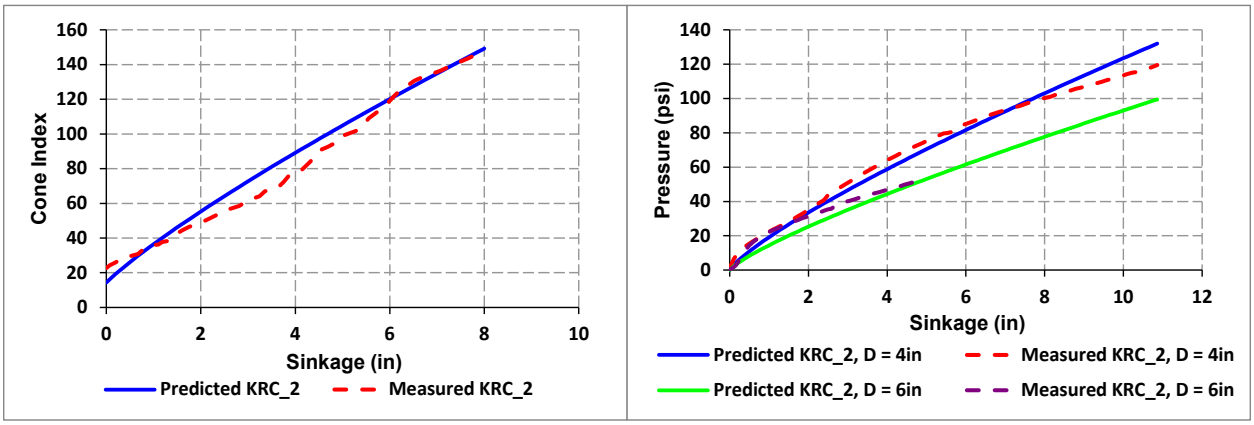

(a) (b)

Figure 4-4. KRC_2 measured and predicted: (a) CI-sinkage relationships; (b) P-S relationships for 4 in. (10 cm) and 6 in. (15 cm)-diameter plates.

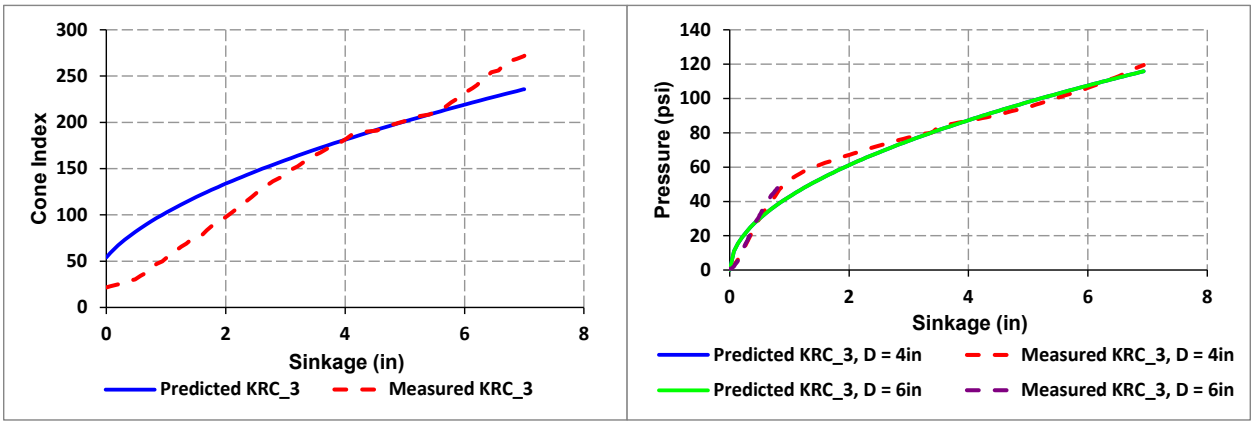

(a) (b)

Figure 4-5. KRC_3 measured and predicted: (a) CI-sinkage relationships; (b) P-S relationships for 4 in. (10 cm) and 6 in. (15 cm)-diameter plates.

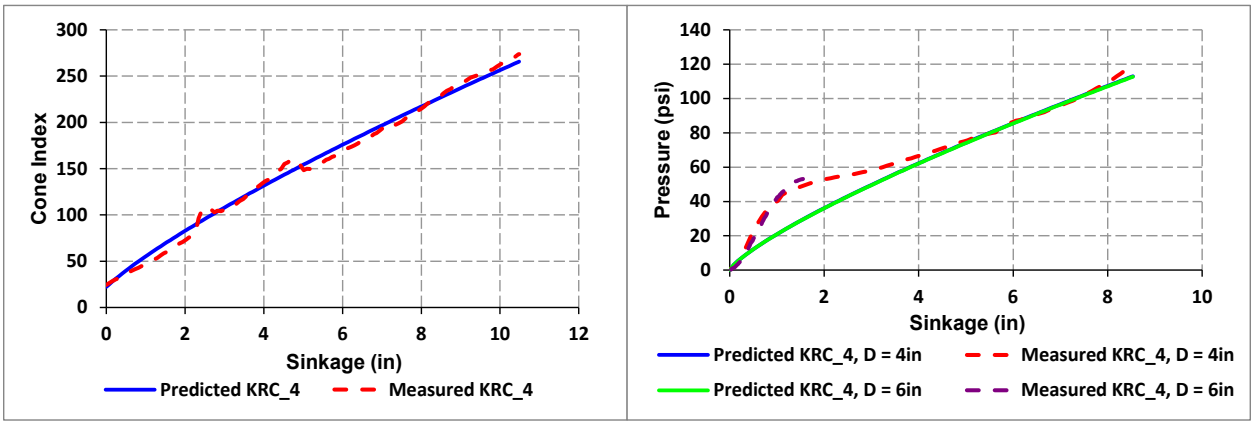

(a) (b)

Figure 4-6. KRC_4 measured and predicted: (a) CI-sinkage relationships; (b) P-S relationships for 4 in. (10 cm) and 6 in. (15 cm)-diameter plates.

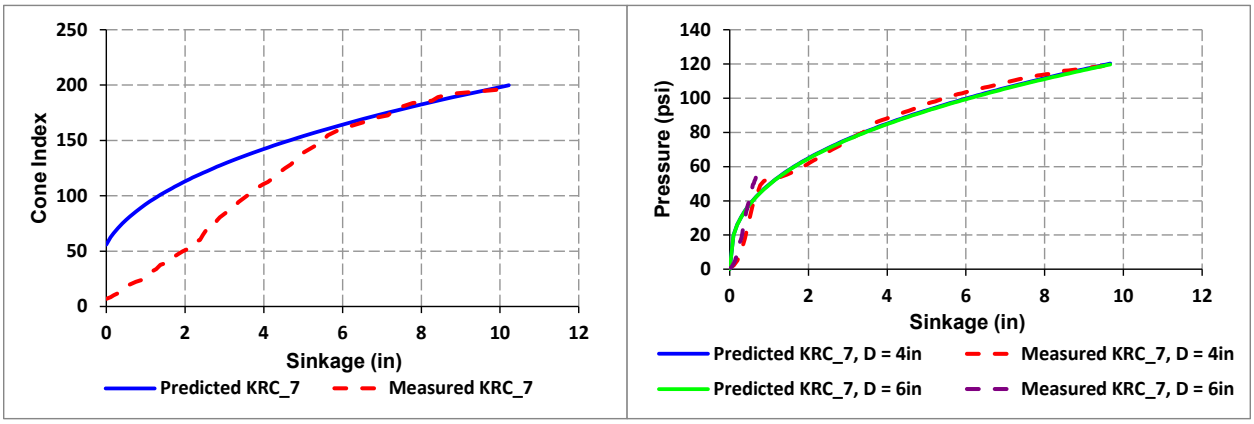

(a) (b)

Figure 4-7. KRC_7 measured and predicted: (a) CI-sinkage relationships; (b) P-S relationships for 4 in. (10 cm) and 6 in. (15 cm)-diameter plates.

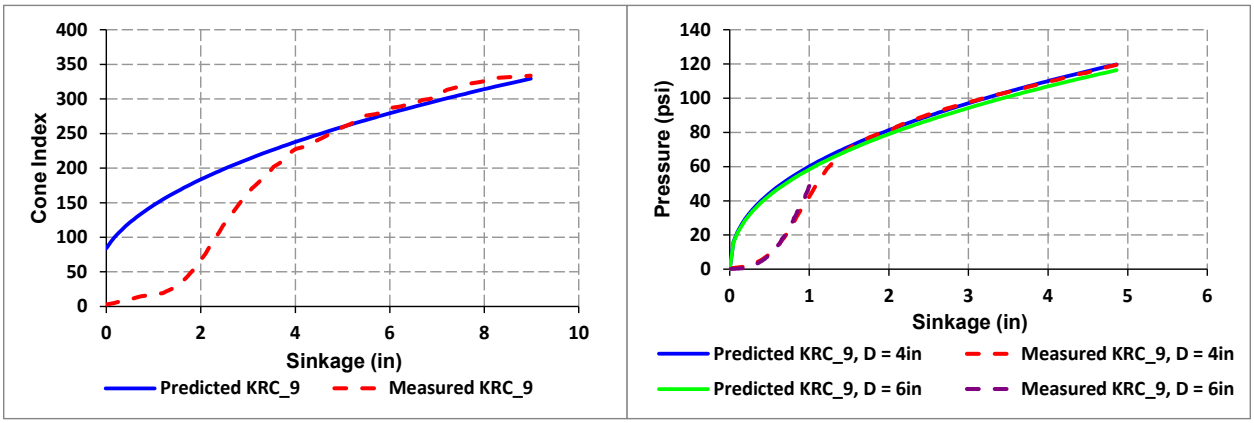

(a) (b)

Figure 4-8. KRC_9 measured and predicted: (a) CI-sinkage relationships; (b) P-S relationships for 4 in. (10 cm) and 6 in. (15 cm)-diameter plates.

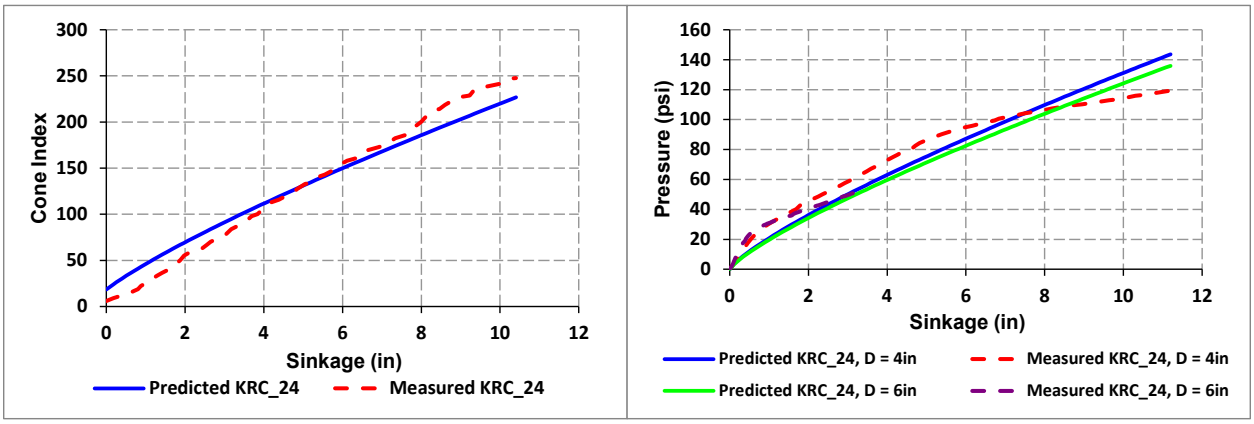

(a) (b)

Figure 4-9. KRC_24 measured and predicted: (a) CI-sinkage relationships; (b) P-S relationships for 4 in. (10 cm) and 6 in. (15 cm)-diameter plates.

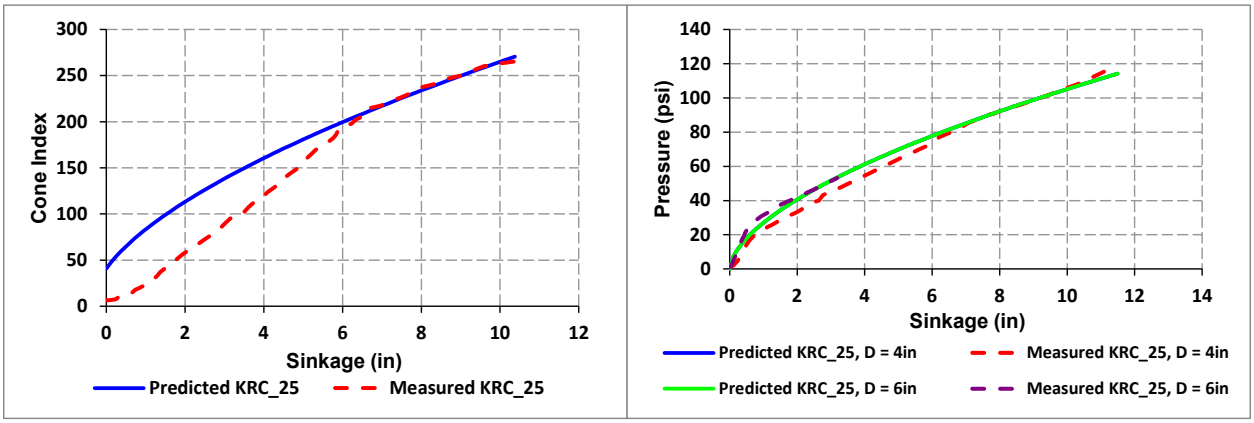

(a) (b)

Figure 4-10. KRC_25 measured and predicted: (a) CI-sinkage relationships; (b) P-S relationships for 4 in. (10 cm) and 6 in. (15 cm)-diameter plates.

To evaluate the goodness of fit between predicted and measured KRC soil P-S relationships, values of R, R^2, RMSD and CV are shown in Table 4-4. The first row, identified as KRC_1, compares the predicted P-S relationships that were derived from the measured CI data on that site with the measured P-S data that was measured on the same site. The remaining seven rows do the same for the other remaining sites. As mentioned previously, the terrain was expected to be different on each of the sites, and hence no attempt was made to compare predictions from one site to measurements from another site.

Table 4-4
R, R^2, RMSD and CV between KRC soil measured P-S relationships and predicted P-S relationships derived from measured CI data.

Data Set	D = 4 in. (10 cm)					D = 6 in. (15 cm)				
	R	R^2	RMSD		CV	R	R^2	RMSD		CV
			kPa	psi				kPa	psi	
KRC_1	0.9952	0.9904	30.47	4.42	0.0573	0.9389	0.8815	48.19	6.99	0.1762
KRC_2	0.9947	0.9895	37.09	5.38	0.0738	0.9881	0.9763	55.92	8.11	0.2413
KRC_3	0.9886	0.9774	31.10	4.51	0.058	0.9835	0.9672	50.47	7.32	0.2522
KRC_4	0.9818	0.964	64.19	9.31	0.1343	0.9928	0.9857	113.5	16.46	0.5486
KRC_7	0.9916	0.9832	32.34	4.69	0.0541	0.9581	0.9179	79.77	11.57	0.4569
KRC_9	0.98	0.9604	92.60	13.43	0.1748	0.861	0.7413	193.9	28.13	1.7126
KRC_24	0.979	0.9584	74.05	10.74	0.1328	0.9726	0.9459	45.23	6.56	0.1844
KRC_25	0.9974	0.9948	31.03	4.5	0.0654	0.9877	0.9756	19.17	2.78	0.0784

It is noted that in a small number of cases, such as that for KRC_9 with D=6 in. (15 cm), the value of the coefficient of determination R^2 is not as high as those for other cases. This is primarily due to the fact that the terrain for KRC_9 is a two-layered one and that the original Bekker equation may not be the most suitable one for characterizing its P-S relationships.

5. Conclusions and Recommendations for Future Developments

5.1. Conclusions

A. An improved cone-terrain interaction model has been developed, which takes into account both normal pressure and shear stress distributions on the cone-terrain interface. This provides an improved way of establishing the relationship between the Cone Index (CI) and the Bekker-Wong terrain parameters in general and that between the Cone Index and the Bekker pressure-sinkage parameters and the cone-terrain shear parameters for this study in particular.

B. A new methodology based on derivative-free optimization algorithms (DFOA) has been developed in combination with the improved cone-terrain interaction model to make use of continuously measured CI vs. sinkage data as input, to predict the three Bekker P-S parameters, k_c, k_ϕ and n, and the two cone-terrain shear parameters, c_c and ϕ_c (the shear deformation parameter K_c for the cone-terrain interface is found to have little effect on the optimization process in the application of DFOA and is therefore omitted in this study).

C. The ability of the DFOA-based methodology and the improved cone-terrain interaction model to predict the Bekker P-S parameters and the cone-terrain shear parameters has been demonstrated for LETE sand and KRC soil data sets, where continuous CI vs. sinkage and bevameter plate pressure-sinkage measurements were both available to provide validations. The correlations between the predicted pressure-sinkage relationships based on the parameters derived from continuous CI-sinkage measurements and that measured are generally encouraging, as evidenced by the values of the coefficient of correlation R, coefficient of determination R^2, root mean squared deviation RMSD, and coefficient of variation CV.

5.2. Recommendations for Future Developments

While the results obtained using the DFOA-based methodology presented in this report are very encouraging, they are of a preliminary and exploratory nature. To further develop the methodology, the following recommendations are made:

A. When the DFOA-based methodology and the improved cone-terrain interaction model are used together to obtain the Bekker P-S parameters and the cone-terrain shear parameters from continuous CI-sinkage measurements, they are critically dependent on having a pressure-sinkage model that is representative over a much broader range of plate sizes than has typically been available in the past. To address this challenge, future bevameter plate size investigations need to be performed over the complete range of plates from vehicle sized (e.g., b=3 in. (7.6 cm) in the Bekker equation), down to the cone base (b=0.4 in. (1 cm)), and, if practicable, even smaller. These tests appear to be straightforward to conduct and will provide critical information about the validity of the estimates of pressure at small plate sizes and will help to validate the RM1 model that was used in the DFOA-based methodology on the LETE sand and KRC soil data.

B. Future combined cone and bevameter tests should be expanded to include metal-terrain shear strength characteristics, to determine if the improved cone-terrain interaction model is a reasonable representation of cone-terrain interaction, and that the DFOA-based methodology obtains reasonable values of cone-terrain shear strength parameters.

C. Future combined cone and bevameter tests should also be expanded to include tests for determining other Bekker-Wong terrain parameters for various types of terrain of interest. These include repetitive loading parameters, terrain internal shear parameters (with tests using a cone coated with a rough grit or with sand particles), rubber-terrain shear parameters (with tests using a cone coated with rubber), and vehicle belly-terrain shear

parameters (with tests using a cone made of the same metal as the vehicle belly and with the same surface conditions (e.g., paint or other coating, roughness, etc.)).

D. To enhance the learning process of the DFOA-based methodology for searching the optimal values of cone-terrain shear parameters, data on shearing characteristics of various cone surfaces (metal surface, surface coated with rough grit, surface coated with rubber, etc.) interacting with a variety of terrains should be collected.

E. In the KRC soil test data set, the terrain behaviour at a given vehicle test site was measured by a single CI vs. sinkage measurement, one pair of plate pressure-sinkage experiments that led to a single set of P-S parameters, and one group of shear stress-shear displacement experiments that led to single set of shear strength parameters. For future combined cone and bevameter tests, it would be extremely valuable if at least three sets of measurements could be made at each test location to assess the repeatability of the measurements, and if the measurements could be made at three or more geographic locations in each vehicle test site to assess the geographic variability of the terrain within the test site.

F. Future CI vs. sinkage measurements should be continuous and should be made from the first point of contact of the cone tip with the terrain, rather than when the cone base is level (or flush) with the terrain surface, in order to provide a more complete set of CI data.

G. The KRC soil PS measurements were limited to 1,500 lb (6,672 N) of vertical force, and hence to 53 and 119 psi (366 and 820 kPa) on the 6 in. (15 cm) and 4 in. (10 cm) diameter plates used in the tests, respectively. The results obtained using 4 in. (10 cm) diameter plate showed a number of significant layers that existed at pressures between 53 and 119 psi (366 and 820 kPa). Since these layers were not measured with both plates, it was impossible to define Bekker P-S parameters that represented the soil behaviour in this 53 -

119 psi (366 - 820 kPa) range. This range is typically of great significance for wheeled vehicles operating in an off-road environment. If KRC conducts further tests, it would be valuable if they could increase the force capability of their bevameter, or make use of smaller plate pairs (e.g., 2.5 and 4 in. (6.4 and 10 cm) diameter).

H. The implementation of the above-noted recommendations would enhance the methodology described herein for predicting the complete set of Bekker-Wong terrain parameters from continuous CI vs. sinkage measurements.

Acknowledgements

The study described in this paper was performed by Vehicle Systems Development Corporation (VSDC), Toronto, Ontario, Canada, as Contractor, and the National Research Council Canada - Automotive and Surface Transportation (NRC-AST), Ottawa, Ontario, Canada, as Subcontractor to VSDC, under Contract No. W911NF-11-D-0001 DO#0417, administered by Battelle Memorial Institute, Columbus, Ohio, for the U.S. Army CCDC Ground Vehicle Systems Center, Warren, Michigan, U.S.A.

Disclaimer

Reference herein to any specific commercial company, product, process or service by trade name, trademark, manufacturer, or otherwise, does not necessarily constitute or imply its endorsement, recommendation, or favouring by the United States Government or the Department of the Army (DoA). The opinions of the authors expressed herein do not necessarily state or reflect those of the United States Government or the DoA and shall not be used for advertising or product endorsement purposes.

6. References

Bekker, M.G., 1969. Introduction to Terrain-Vehicle Systems. The University of Michigan Press, Ann Arbor, Michigan, U.S.A.

Davis, L., 1991. Handbook of Genetic Algorithms. Van Nostrand Reinhold, New York, U.S.A.

Gerth, R., Bradley, S., Letherwood, M. and Gorsich, D., 2019. The data used in next generation NATO reference mobility model cooperative demonstration of technology. in: 2019 NDIA Ground Vehicle Systems Engineering and Technology Symposium, Novi, Michigan, U.S.A. Manuscript submitted for publication.

Goldberg, D., 1989. Genetic Algorithms in Search, Optimization and Machine Learning. Addison-Wesley, Boston, Massachusetts, U.S.A.

Janosi, Z., 1959. Prediction of "WES Cone Index" by means of a stress-strain function of soils. Land Locomotion Laboratory, U.S. Department of the Army, Ordnance Tank-Automotive Command, Research Division, Report No. 46.

Janosi, Z. and Hanamoto, B., 1961. The analytical determination of drawbar pull as a function of slip for tracked vehicles in deformable soils. in: Proc. of the 1st International Conference on the Mechanics of Soil-Vehicle Systems, Edizioni Minerva Tecnica, Torino, Italy, 707-736.

Kennedy, J. and Eberhart, R., 1995. Particle Swarm Optimization. in Proc. of IEEE International Conference on Neural Networks. IV, 1942-1948.

Kennedy, J., 1997. The particle swarm: social adaptation of knowledge. In: Proc. of IEEE International Conference on Evolutionary Computation, 303-308.

Kennedy, J. and Eberhart, R., 2001. Swarm Inteligence. Morgan Kaufmann, Burlington, Massachusetts, U.S.A.

Mitchell, M., 1998. An Introduction to Genetic Algorithms. MIT Press, Cambridge, Massachusetts, U.S.A.

Shi, Y. and Eberhart, R., 1998. A modified particle swarm optimizer. In Proc. of IEEE International Conference on Evolutionary Computation, 69-73.

Wilson, E.O., 1975. Sociobiology: The new synthesis. Belknap Press, Cambridge, Massachusetts, U.S.A.

Wong, J.Y., 1981. Field measurements of the mechanical properties of a sandy terrain at LETE. Transport Technology Research Laboratory, Carleton University, Report No. FM-82-SA, prepared for Defence Research Establishment Suffield, Department of National Defence, Canada.

Wong, J. Y., 1992. Optimization of the tractive performance of articulated tracked vehicles using an advanced computer simulation model. Proc. Inst. Mech. Eng., Part D, J. Autom. Eng. 206 (D1), 29-45.

Wong, J.Y., 1995. Application of the computer simulation model NTVPM-86 to the development of a new version of the infantry fighting vehicle ASCOD. J. Terramech. 32 (1), 53-61.

Wong, J.Y. and Huang, Wei, 2006. Study of detracking risks of track systems. Proc. Inst. Mech. Eng., Part D, J. Autom. Eng. 220, 1235-1253.

Wong, J.Y. and Asnani, V.M., 2008. Study of the correlation between the performance of lunar vehicle wheels predicted by the Nepean wheeled vehicle performance model and test data. Proc. Inst. Mech. Eng., Part D, J. Autom. Eng. 222, 1939-1954.

Wong, J.Y., 2008. Theory of Ground Vehicle, 4th Edition. John Wiley, New Jersey, U.S.A.

Wong, J.Y., 2010. Terramechanics and Off-Road Vehicle Engineering, 2nd Edition. Elsevier, Oxford, England.

Wong, J.Y., Senatore, C., Jayakumar, P., Iagnemma, K., 2015. Predicting mobility performance of a small, lightweight track system using the computer-aided method NTVPM. J. Terramech. 61, 23-32.

Wong, J.Y., Jayakumar, P., Toma, E., Preston-Thomas, J., 2018. Comparison of simulation models NRMM and NTVPM for assessing military tracked vehicle cross-country performance. J. Terramech. 80, 31-48.

Wong, J.Y., Jayakumar, P., Preston-Thomas, J., 2019. Evaluation of computer simulation model NTVPM for assessing military tracked vehicle cross-country mobility. Proc. Inst. Mech. Eng., Part D, J. Autom. Eng. 233 (5), 1194-1213.